THE JOURNAL OF NAVIGATION (2007), **60**, 349–362. © The Royal Institute of Navigation
doi:10.1017/S0373463307004365 Printed in the United Kingdom

THE JOURNAL OF NAVIGATION

VOL. 60 SEPTEMBER 2007 NO. 3

GPS Receiver Demonstration on a Galileo Test Bed Satellite

Takuji Ebinuma

(*Surrey Space Centre*, *University of Surrey*)

Martin Unwin

(*Surrey Satellite Technology Ltd*)
(Email: M.Unwin@sstl.co.uk)

GPS receivers have been used successfully on low Earth orbit (LEO) satellite missions for several years. The use of a GPS receiver at altitudes higher than LEO, however, is non-trivial as the receiver will be outside the main lobe of the GPS broadcast signals, and it will have to track signals from GPS satellites transmitting from the other side of the Earth. This paper will review the special hardware and software adaptations required for GPS receiver operations on a medium Earth orbit or geostationary satellite, along with preliminary results from simulations and an in-orbit experiment.

KEY WORDS

1. GPS. 2. Galileo. 3. Geostationary satellite.

1. INTRODUCTION. In collaboration with European Space Agency (ESA), Surrey Satellite Technology Ltd (SSTL) was given the opportunity to manufacture one of the first Galileo demonstration satellites. SSTL built the Galileo System

Test Bed V2/A (GSTB-V2/A) satellite, later renamed as GIOVE-A, in parallel with the GIOVE-B satellite being built by Galileo Industries (Rooney, *et al*., 2004). The primary goals of the GIOVE missions are to secure the international frequency allocation for Galileo and to validate key technologies for the full Galileo constellation.

In addition to the main navigation payloads, GIOVE-A also carries a laser retroreflector array to permit coordinated tracking by the international satellite laser community and the precise recovery of the orbit. Furthermore, an experimental GPS receiver is carried for a demonstration of an alternative technique for orbit determination for medium Earth orbit (MEO) and geostationary (GEO) satellites. This receiver is an adaptation of the SGR-GEO GPS receiver currently under development within SSTL to provide a GPS receiver suitable for use on GEO missions.

As spacecraft altitude increases the condition for the reception of GPS signals becomes less favourable. The receiver has to track weaker signals from GPS satellites positioned on the far side of the Earth. At GEO altitudes, this signal illuminates only a small portion of the orbit, and the Earth blocks out a significant portion of the available signal window. Therefore the GPS main lobe signals subtend only a small annular region of the GEO orbit. This gives poor satellite geometry and very few visible satellites. In fact, satellite visibility will be slightly worse in MEO as the arc of GPS visibility will be shorter than GEO. The satellite selection algorithm of the receiver will be modified accordingly, and a higher gain and efficiency antenna is used to reduce those effects.

The GPS baseband processor used on SGR-GEO is the GP4020 chip of the Zarlink Semiconductor. This provides similar performance to the GP2021 correlator and ARM60B microprocessor used on SGR-10/20 receiver (Unwin and Oldfield, 2000), but with lower power consumption. The receiver hardware will be exposed to much higher radiation in MEO/GEO. Early radiation dose testing indicates that the SGR-GEO receiver will need substantial radiation shielding as well as Error Detection and Correction (EDAC) and latch-up protection switches (Underwood, *et al*., 2004), but its small size minimises the shielding material required. The material used for the antenna has also to be selected carefully to minimise dielectric and surface charging risk.

In this SGR-GEO demonstration on the GIOVE-A satellite, the GPS measurements are recorded and downloaded to a ground station for post-processed orbit recovery. SSTL's orbit estimator for LEO microsatellite orbit determination is being adapted for MEO/GEO applications. Future improvements toward a practical SGR-GEO product include weak signal acquisition and tracking. The weak signal capability is intended to increase the number of satellite visible through the tracking of side lobes of the GPS satellite antennas. An early study suggests that four or more satellites are visible in GEO for approximately 85% of the time when including the GPS side lobe signals (Moreau, *et al*., 2000). However, signals in the side lobes are believed to be 15–20 dB lower than the main signals and would not be detectable with a normal GPS receiver. Major software modifications are required to improve the signal sensitivity. The SGR-GEO will use the weak signal tracking method proposed by Akos, *et al*. for their software GPS receiver design (Akos, *et al*., 2000). The idea is to use two successive sets of 10 ms correlation data within the 20 ms data prediction time interval. This guarantees that at least one of those data sets does not contain a data bit transition of the navigation data and provides 10 dB more signal gain over a

typical 1 ms correlation time interval. The preliminary test results show that the SGR-GEO is capable of tracking the weak signals as low as 24 dB-Hz C/N_0.

The use of a GPS receiver above the GPS constellation has been discussed in various papers, but only a few flight experiments have been flown (Coulson and Shave, 1996; Balbach, *et al*., 1998; Bandecchi and Ockels, 1998; Powell, *et al*., 1999; Cronman, 2000). The most significant one is probably the NASA GPS experiment on AMSAT OSCAR-40 (AO-40) satellite, where the reception of GPS side-lobe signals was demonstrated using a Trimble TANS receiver with LEO heritage (Moreau, *et al*., 2002). The SGR-GEO experiment is the first civil flight of a GPS receiver that has been specially designed for the MEO/GEO orbit, including weak signal acquisition and tracking.

2. SGR-GEO RECEIVER DESIGN.

The SGR-GEO design is a successor to the design of the SGR-10 and SGR-20 produced by SSTL and flown successfully on a number of LEO satellites (Unwin and Oldfield, 2000). The earlier SGR design was based on the Zarlink Semiconductor (formerly Mitel and GE Plessey) GP2000 GPS chipset series, while the new SGR-GEO is based upon the GP4020. This requires a new hardware design, but the receiver firmware can be readily ported across from the earlier SGRs.

A number of new features are included in the design to optimise for space use, and specifically for use at MEO/GEO altitudes:

- Medium gain passive patch antenna
- Protection circuitry in low noise amplifier (LNA)
- Additional radiation shielding
- Error detection and correction (EDAC) for the receiver's memory
- Latch-up protection circuitry
- Oven controlled crystal oscillator (OCXO)
- Ferro-electric random access memory (FRAM)
- Additional 12 channels of correlators
- Onboard analog-to-digital (A/D) converter

2.1. *Antenna and LNA Design*.

The antenna is a new design commissioned from European Antennas Ltd. It is designed to have a medium gain, 6 or 7 dBi, while retaining a wide beamwidth. An air-gap patch design was initially envisaged not only to achieve higher efficiency, but also to address the danger of dielectric charging at MEO/GEO altitudes. However, it was felt that tolerance to launch vibration loads required a supporting dielectric, so a dielectric has been chosen with a very low density Rohacell form. The antenna carries a parasitic element that is thickened to provide additional shielding of the dielectric from electrons.

The SGR-GEO receiver is designed to acquire GPS signals which happen to be the same frequency as the Galileo E1 signal transmitted by the GIOVE-A satellite. Thus the input filters in the LNA and receiver will offer no protection to these powerful broadcast signals, and the total Galileo signal transmit power is easily high enough to destroy the GPS LNA and possibly the receiver too. The risk of signals damaging the GPS LNA and the receiver has been addressed by incorporating some protection circuitry in front of the LNA, using PIN and Schottky diodes. When no transmit

signals are present, these diodes remain switched off, and only cause a marginal increase in noise figure in the receiver system. When powerful transmit signals appear, the diodes are self-biased and protect the subsequent LNA and receiver circuitry. It is quite likely that the protection circuit will never be activated, but the presence of this circuitry should give assurance that the receiver is safe in all circumstances.

2.2. *Radiation Mitigation.* An early study suggested that the total dose of the GP4020 is acceptable for LEO applications, as a lifetime of longer than 10 years is foreseen under average conditions, given 4 mm aluminium screening (Underwood, *et al.*, 2004). The receiver could also be used in higher orbits, e.g. GEO, given extensive shielding. If an equivalent of 10 mm of aluminium is used, it is calculated that the receiver will survive 7–10 years in GEO.

The same study showed that the single event upset (SEU) susceptibility is a matter of concern, as a significant number of upsets are to be expected especially in LEO. The entire RAM external to the GP4020 will be triple modular redundancy (TMR) EDAC protected. This method of EDAC provides protection against SEUs without the overhead of a wait state, unlike the other methods. The GP4020 internal RAM, which is not protected, is only used sparingly if at all. It is not possible to avoid using the registers but the chances of register upset that causes a functional effect should be small enough to achieve an acceptable degree of robustness.

It is also observed that the single event latch-up rate is sufficiently low. As with the other SGR receivers, a latch-up switch will be used to switch the receiver off rapidly after any current surge. SSTL's latch-up switch has been flown on several missions and was also proven during the radiation test campaign.

2.3. *OCXO.* The standard SGR receiver obtains its frequency reference from a temperature compensated crystal oscillator (TCXO). The frequency error of the TCXO is estimated and corrected as part of velocity fix solutions. In MEO/GEO, however, the GPS receiver will experience long periods where no GPS signals are tracked. During these outages, the receiver will coast until signals are tracked again. The stability of a TCXO is not good enough to maintain the time in the receiver with sufficient accuracy therefore an OCXO will be used on SGR-GEO instead. The OCXO has little or no temperature dependency and its dynamics can be more easily modelled.

2.4. *Other Receiver Electronic Design Aspects.* The SGR-GEO receiver hardware is built around Zarlink's GP4020 GPS baseband processor, which includes an integrated ARM7 processor with a 12-channel correlator. An additional 12 channels are provided by the GP2021 correlator, potentially allowing for rapid signal acquisition using a parallel search on 24 channels.

As with the early SGR design, a battery-backed non-volatile RAM is being avoided to ensure that all latch-ups can be caught and reset immediately. Instead, a FRAM will be used on the SGR-GEO receiver. FRAM reportedly has a higher tolerance to radiation than FLASH memory and, more importantly, avoids the risk of single-event burn-out when programming under radiation. The FRAM block cannot maintain a real-time clock, but will be able to maintain copies of GPS Almanac, broadcast Ephemeris, and user orbital elements during power cycling, and will permit faster signal acquisition than from cold start.

An A/D converter is also included to permit the measurement of temperature and currents on the board.

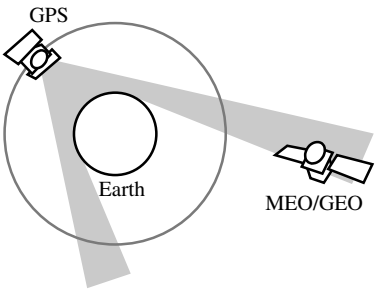

Figure 1. GPS signal visibility at MEO/GEO altitudes.

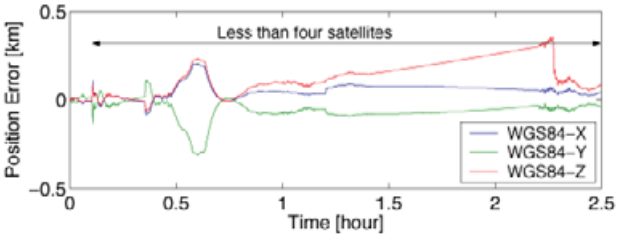

Figure 2. Orbit estimator performance when less than four GPS satellite are visible.

3. RECEIVER OPERATIONS. The MEO/GEO altitudes provide a very unfavourable environment for the reception of GPS signals. The receiver has to track signals from GPS satellites positioned on the far side of the Earth, as illustrated in Figure 1. The main lobe of the GPS L1 signal has a half-beamwidth of 21·3°. At the GEO altitude, this signal illuminates only a small portion of the orbit. Additionally the Earth blocks out a significant portion of the available signal window about a half-width of 13·9°. This exclusion angle could be increased further to avoid signal paths traversing the densest parts of the atmosphere. Therefore, the GPS signals subtend only a small annular region of the GEO orbit.

The geometry is similar for a GPS receiver on an MEO satellite. In fact, the situation will be slightly worse as the arc of GPS visibility will be shorter at MEO than GEO. Initial analysis on the visibility of GPS satellites from the GIOVE-A orbit suggests that four or more GPS satellites are in view for approximately ten percent of the time. As standard GPS navigation solutions can only be generated when at least four satellites are being tracked, an alternative method is required to generate position solutions over the majority of the GIOVE-A orbit using underdetermined GPS measurements.

To overcome this problem, SSTL's orbit estimator for LEO microsatellites is being adapted for MEO/GEO applications. The baseline operation of the GPS experiment on GIOVE-A is to acquire GPS pseudorange and Doppler measurements and downlink these data to be processed on the ground. Once the performance and processing requirements of the orbit estimator have been validated, then further experiments may be possible to investigate the integration of the estimator into the receiver to provide autonomous in-orbit operations. Figure 2 shows typical GIOVE-A orbit

https://doi.org/10.1017/S0373463307004365 Published online by Cambridge University Press

estimation accuracy when less than four satellites are visible. This preliminary simulation result suggests that the estimator is capable of providing better than 500 m position accuracy even when position fix solutions are not available.

The orbit estimator simulation results also suggest that the lack of knowledge of the behaviour of the receiver clock would be a significant problem. Since position fix solutions are rarely available in MEO/GEO orbits, the time and frequency offsets of the receiver clock may never be determined preventing meaningful interpretation of the receiver measurements. The same problem was also reported by NASA Goddard Space Flight Center from experiences with their GPS experiment on the AO-40 satellite (Moreau, *et al*., 2002).

The receiver time offset can be initialised within a few milliseconds of the actual GPS system time by assuming that coarse receiver position information, e.g. a Two-Line Element (TLE) set of GIOVE-A, is available. At the reception of the hand over word (HOW) of the GPS broadcast navigation message, the receiver clock, t_R, can be initialised by:

$$t_R = t_{HOW} - \frac{d}{c} \tag{1}$$

where t_{HOW} is the satellite signal transmission time embedded in the HOW, c is the speed of light, and d is the approximate range between the GPS satellite and the receiver. Many commercial GPS receivers, including the Trimble TANS receiver used on the AO-40 satellite, are designed for terrestrial applications and simply assume a fixed signal propagation time, d/c, of typically 0·07 seconds. The SGR-GEO receiver, on the other hand, utilises the TLE of the user satellite and GPS broadcast Ephemeris to compute the signal propagation time and is capable of initialising the receiver clock time within a few milliseconds of the actual GPS system time. This small clock error is inherited by measurement time tag and if not accounted for, causes less than 5-metre positioning offset in the along track directions due to a high orbiting velocity of the MEO/GEO satellite. Once at least four satellites have been acquired, the receiver clock is corrected very precisely using a position fix solution. The OCXO used on the SGR-GEO receiver will provide little or no temperature dependency and a more stable reference frequency than a TCXO.

The TLE of the user satellite can also be used to forecast satellite visibility for channel allocation and predict the Doppler shift for signal search.

4. ENHANCED SOFTWARE DESIGN.

A weak signal acquisition and tracking capability has been investigated as part of enhanced design toward practical SGR-GEO operations. The signal acquisition process involves searching over the full range of code delays and Doppler frequencies to find the signals present in the noise. Once coarse code delay and Doppler frequency are found, the tracking loops use feedback from discriminators to make more accurate estimates of the delay and carrier Doppler. These parameters are then used to form the pseudorange and Doppler measurements.

Figure 3 shows the correlator block diagram of a typical GPS receiver. The code mixer multiplies a local replica code to incoming baseband signal. If the replica code matches the incident signal, the signal is despread and a carrier signal is recovered. The carrier mixers multiply the sine and cosine versions of the local carrier

https://doi.org/10.1017/S0373463307004365 Published online by Cambridge University Press

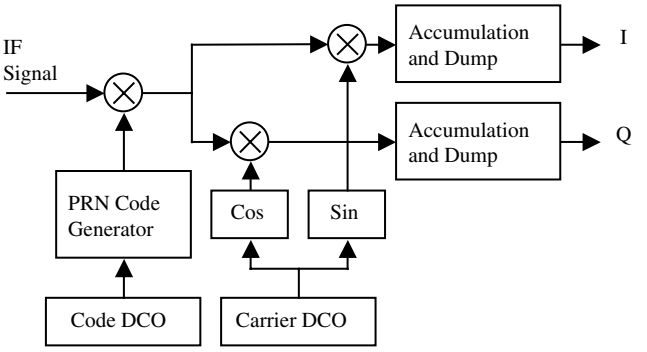

Figure 3. GPS correlator block diagram.

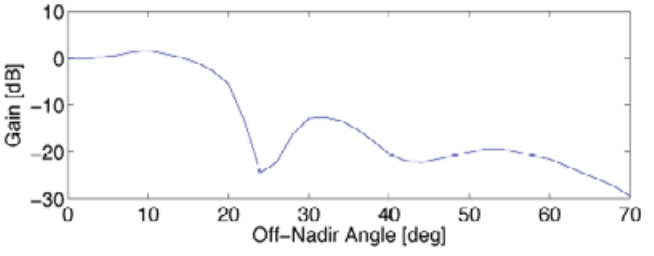

Figure 4. Typical GPS transmitter antenna gain pattern.

signal controlled by a digitally controlled oscillator (DCO). The Accumulate and Dump blocks integrate the mixer outputs over a complete code period of normally 1 ms. There are two accumulators for each code generator. These represent the correlation of the in-phase (I) and quadrature (Q) components over the integration period.

The weak signal capability is intended to dramatically increase the number of satellites visible through the tracking of side lobes of the GPS satellite antennas. Signals in the side lobes are believed to be 15–20 dB lower than the main signals (Czopek and Shollenberger, 1993) as shown in Figure 4 and would not be detectable with a normal GPS receiver, but can be tracked using a longer coherent integration of the I and Q components.

However, several obstacles prevent a longer coherent process in conventional receivers. One of the biggest obstacles is the navigation message, which is a continuous 50 Hz data stream modulated onto the GPS signal. As the two data bits may have opposite polarity, coherent integration across a data bit edge could be zero. Thus, coherent integration of longer than 20 ms requires knowledge of the navigation message beforehand. Akos, *et al.* suggested a method to increase the coherent integration interval without identifying the bit edge of the navigation data (Akos, *et al.*, 2000). This method simply divides each 20 ms navigation bit interval into two 10 ms data sets, A and B, as shown in Figure 5. This guarantees that at least one of those data sets does not contain a data bit transition of the navigation data and provides

https://doi.org/10.1017/S0373463307004365 Published online by Cambridge University Press

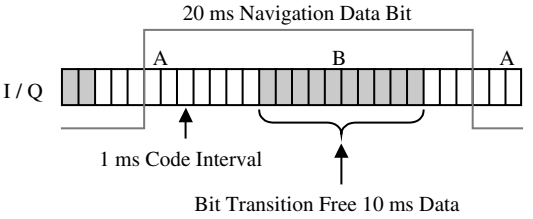

Figure 5. Two 10 ms coherent integration data sets and navigation bit.

10 dB more signal gain over a typical 1 ms correlation time interval. The coherently integrated correlation components are expressed by:

$$\begin{cases} I_A = \sum_{k=1}^{10} I_k \\ Q_A = \sum_{k=1}^{10} Q_k \end{cases}, \text{ and } \begin{cases} I_B = \sum_{k=11}^{20} I_k \\ Q_B = \sum_{k=11}^{20} Q_k \end{cases} \tag{2}$$

4.1. *Weak Signal Acquisition*. GPS signal acquisition is a two dimensional search in which a replica code and carrier are aligned with the received signal. The correct alignment is identified by measurement of the output power of the correlators. When both the code and carrier Doppler match the incident signal, the magnitude of the output power of the correlator is at a maximum. Given the code delay and Doppler, the receiver checks if the correlator exceeds a predefined threshold. If this fails, the search is continued in another set of code delay and Doppler trial values.

The signal acquisition threshold is generally higher then the tracking threshold, mainly because of possible correlation power loss due to code phase and carrier frequency errors. To achieve a lower signal acquisition threshold, the 10 ms coherent integration results are then combined incoherently, i.e. the correlation powers of coherent integration blocks are summed. The SGR-GEO weak signal acquisition process integrates 10 sets of 10 ms coherent correlation powers. Earlier study shows that a 10 times longer incoherent integration results in about a 5 dB increase in sensitivity (Winternitz, *et al*., 2004). The incoherently integrated correlation powers of data sets A and B are expressed by:

$$P_A = \sum_{k=1}^{10} \left(I_{A,k}^2 + Q_{A,k}^2 \right), \quad \text{and} \quad P_B = \sum_{k=1}^{10} \left(I_{B,k}^2 + Q_{B,k}^2 \right) \tag{3}$$

The incoherent integration does not increase the signal level but reduces noise level. This increases the margin between the acquisition threshold and false alarms due to the noise and provides more reliable weak signal acquisition. Figure 6 shows recorded noise signal power of coherent integration only (above) and incoherent integration (below) cases using a single channel GPS signal simulator. It is clear that the incoherent integration process efficiently reduces the noise level.

The signal acquisition threshold is generally 5 dB or more above the expected noise floor, that is around 20 dB-Hz C/N_0 for 10 ms coherent integration time. Figure 7 shows a code search result of a weak signal of 25 dB-Hz C/N_0, which may be

https://doi.org/10.1017/S0373463307004365 Published online by Cambridge University Press

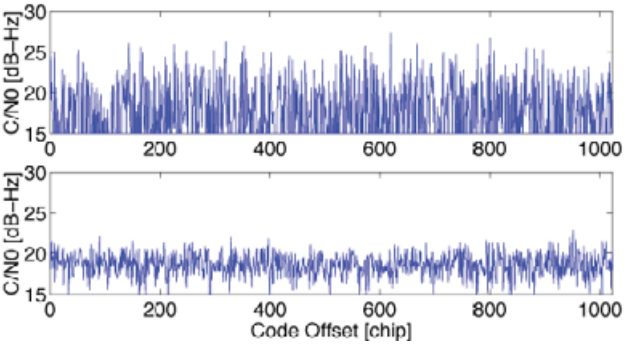

Figure 6. Noise powers of coherent integration only (above) and incoherent integration (below) cases.

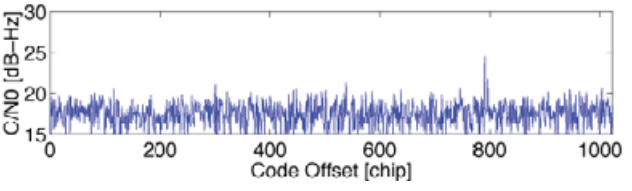

Figure 7. Correlation power peak of 25 dB-Hz C/N_0 signal at code offset of 790 chips.

undetectable by the coherent accumulation only case because of so many false peaks due to noise.

4.2. *Weak Signal Tracking*. Once either of the incoherent integration values exceeds a predefined acquisition threshold, the receiver starts to track the signal. First, the signal tracking process needs to define which coherent integration data set is to be used. The signal power of the one data set containing a navigation message bit transition should be lower than the other. However, there may be no data transition during that 20 ms period, and both data sets will have the same signal power. The noise in the accumulated data also provides erroneous signal power readings. To minimise those effects, the receiver uses a voting scheme, in which it votes the data set A or B if the signal power of one of them is at least 3 dB higher than the other. When the number of votes of either of them exceeds a predefined threshold, the receiver starts tracking signal using that particular data set.

Preliminary testing of the weak signal tracking was conducted with a single channel GPS signal simulator. In this test, the simulator initially provided a reasonably strong signal (40 dB-Hz C/N_0). Once the receiver started tracking the signal, the output power of the simulator was reduced in steps until the receiver lost the lock. Figure 8 shows the C/N_0 readings from the receiver during the test. It successfully tracked the weak signals as low as 24 dB-Hz C/N_0. An early study suggests that four or more satellites are visible in GEO for approximately 85% of the time with tracking threshold of 28 dB-Hz C/N_0 (Moreau, *et al.*, 2000). This means that the SGR-GEO receiver is capable of providing position fix solutions for most of the time in MEO/GEO. An orbit propagator will also be employed by the final SGR-GEO

https://doi.org/10.1017/S0373463307004365 Published online by Cambridge University Press

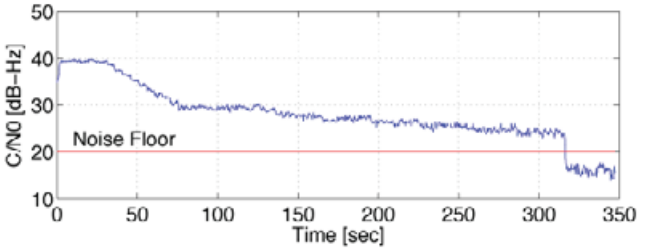

Figure 8. Weak signal tracking test results with the effects of successive reduction of signal power.

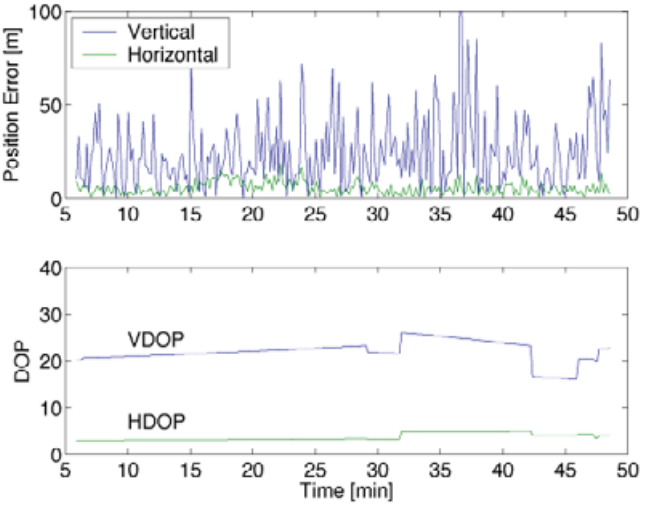

Figure 9. Weak signal point positioning simulation with an MEO scenario.

enhanced software to provide propagated orbit information when the position fix solutions are unavailable.

5. POINT POSITIONING PERFORMANCE. A multi-channel weak signal tracking capability has been implemented to provide code phase measurements for positioning. To verify the new receiver software performance, a series of hardware-in-the-loop simulations using a GPS signal simulator was performed. All the tests were performed using a Spirent STR4760 signal simulator with an MEO scenario of 56° inclination and 30,000 km altitude (midway between GIOVE-A and GEO altitudes).

Figure 9 shows an example weak signal positioning result and corresponding dilution of precision (DOP) values in a 1-hour simulation. It has to be noted that any real-time navigation capability has not yet been implemented, and the position fix solutions were computed by post-processing the recorded code phase measurements. The navigation result exhibits typical position error of 50–100 m in the local vertical (i.e. in the radial) direction and 10–15 m in the local horizontal direction. The

https://doi.org/10.1017/S0373463307004365 Published online by Cambridge University Press

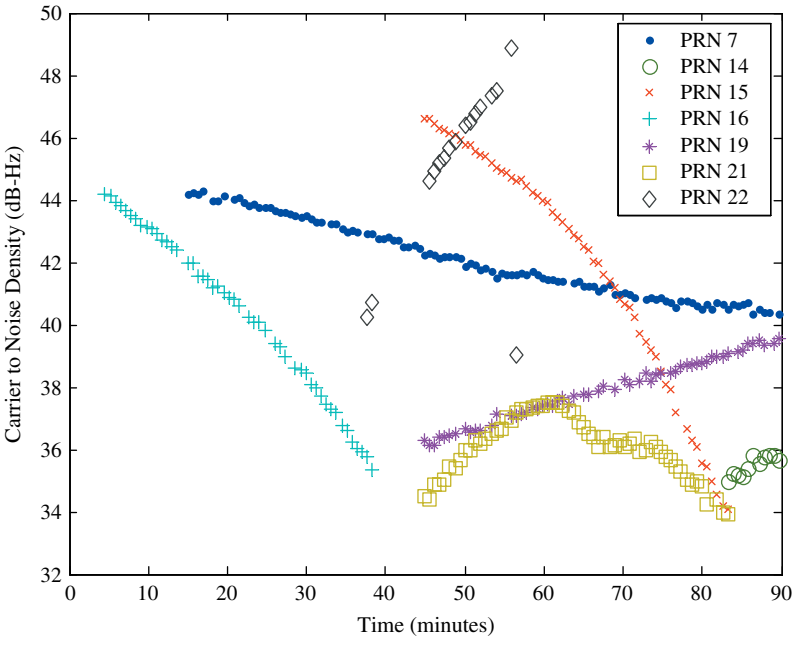

Figure 10. Satellites tracked on 11th May 2006 by SGR-GEO.

position error in the local vertical direction is always 3–5 times larger than that in the horizontal direction due to very poor satellite geometry. Especially, the receiver's unknown clock offset makes it difficult to determine the local vertical position accurately. Although 5–6 satellites were being tracked during the simulation, all of the satellites were always located within 15–25° off-nadir window (i.e. −65° to −75° elevation), which provides a vertical DOP (VDOP) of 15–25 while the horizontal DOP (HDOP) value is generally smaller than 5.

6. PRELIMINARY IN-ORBIT RESULTS. GIOVE-A was launched on 28 December, 2005 and deployment of the solar panels and commissioning of the spacecraft was completed 2 weeks later. This was followed by a period attaining GIOVE-A's primary mission objectives, completing the Galileo frequency filings for submission to the ITU (Falcone *et al.*).

The SGR-GEO was first turned on in orbit on 11 May 2006, with subsequent operations on 12, 16 & 17 May. The objectives of the first two operations were to commission the hardware, ensure that all interfaces were operating correctly post-launch, and to upload the baseline code. About 70 minutes of data was collected on the first operation, during which time the SGR-GEO commenced tracking satellites using its pre-launch code. Seven different satellites were tracked, up to five simultaneously, but unfortunately no position fix was possible due to the premature code configuration. In the subsequent operation, the baseline code was successfully uploaded.

Figure 10 shows the different GPS satellite signals (PRNs) tracked during the first operation. The elevations of the tracked satellites with respect to GIOVE-A were

https://doi.org/10.1017/S0373463307004365 Published online by Cambridge University Press

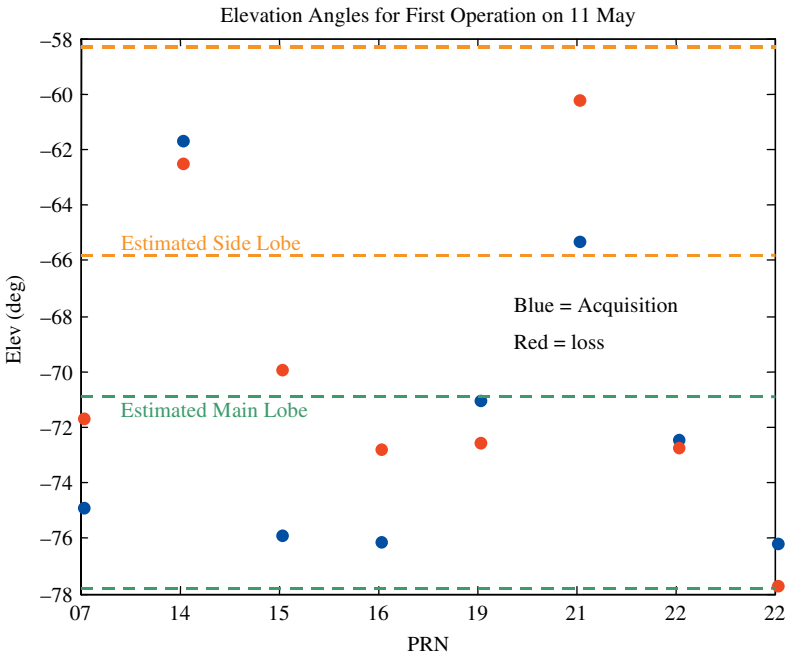

Figure 11. Calculated elevations of GPS satellites tracked by the SGR-GEO.

determined (see Figure 11). This showed that most satellites tracked were within the -78° to -71° (where -90° is nadir) elevation band consistent with the expected elevation for a GPS transmit antenna main lobe signal. PRN 22 appears twice in Figure 11 as the signal was lost after acquisition, and subsequently re-acquired. C/N_0 readings are roughly 4 dB lower than typical for a LEO SGR receiver, which is consistent with the greater distance the signals must travel (roughly twice, giving about 6 dB extra path-loss) and the increased antenna gain on the SGR-GEO (approximately 2 dB increase over standard patch antennas used in LEO). Contrary to expectations, though, side lobe signals were tracked without the need for weak signal tracking algorithms. PRNs 14 & 21 (both Block II-R GPS satellites) are tracked at elevations between -58° and -66°, consistent with elevations expected for the side lobe. This could either indicate that side-lobes are higher than expected or, more likely, side-lobe patterns are quite variable in amplitude with azimuth, and from satellite to satellite. More data is required to examine these patterns.

Two subsequent operations saw the SGR-GEO tracking at most only three satellite mainlobe signals simultaneously in line with predictions. No sidelobe signals were tracked during this brief operation. While not allowing a fully determined navigation fix, the logged pseudoranges are being used to test the Kalman filter orbit estimator and to assist in developing an orbit fitting algorithm for the period that the SGR-GEO was turned on during 16th May.

Unfortunately no further testing of the SGR-GEO has been possible since these first operations as a result of prioritisation conflicts with the main navigation transmission payload. Key demonstrations of Galileo signals and filter compensations are still required and these have been given higher priority by the customer. It is hoped

https://doi.org/10.1017/S0373463307004365 Published online by Cambridge University Press

that later in the mission more operations of the SGR-GEO will be possible, and in particular to demonstrate the weak signal and orbit estimator algorithms for the first time in orbit. More details on the experiment, hardware and preliminary results have been presented elsewhere (Steenwijk *et al*., 2006).

7. CONCLUSIONS. This paper has described the development of a new GPS receiver, SGR-GEO, for future GEO applications. The paper has also reviewed the special adaptation required for MEO/GEO operations including radiation assessment and mitigation, antenna design and OCXO accommodation. The enhanced software of the receiver will also use weak signal acquisition and tracking to increase the number of visible satellites in MEO/GEO orbits. The preliminary test results of the weak signal algorithms suggest that the receiver is capable of tracking weak signals as low as 24 dB-Hz and providing position fix solutions with accuracies of 50–100 m in the local vertical and 10–15 m in the local horizontal directions at an MEO altitude. The SGR-GEO receiver has been carried into orbit for the first time on the GIOVE-A satellite which was launched in December 2005, and preliminary tests have shown the tracking of five GPS satellite signals simultaneously.

ACKNOWLEDGEMENTS

The funding of this work has come from Surrey Space Centre, SSTL, and ESA Ministerial Preparatory Action (EMPA). ESA's support for the flight opportunity on the GIOVE-A satellite is also gratefully acknowledged. Thanks are due to members of the GNSS team at SSTL for assistance with the data processing.

REFERENCES

Akos, D. M., Normark, P. L., Lee, J. T., Gromov, K. G., Tsui, J. B. Y. and Schamus, J. (2000). Low Power Global Navigation Satellite System (GNSS) Signal Detection and Processing. *Proceedings of ION GPS 2000*, Salt Lake City, Utah.

Balbach, O., Eisheller, B., Hein, G. W., Zink, T., Enderle, W., Schmidhuber, M. and Lemke, N. (1998). Tracking GPS Above GPS Satellite Altitude: Results of the GPS Experiment on the HEO Mission Equator-S. *Proceedings of ION GPS 98*, Nashville, Tennessee.

Bandecchi, M. and Ockels, W. J. (1998). The TEAMSAT Experience. *ESA Bulletin*, No. 95.

Cronman, J. D. (2000). Experience Using GPS for Orbit Determination of a Geosynchronous Satellite. *Proceedings of ION GPS 2000*, Salt Lake City, Utah.

Coulson, P. and Shave, N. P. (1996). The GPS at GEO Experiment. *Proceedings of the 3rd ESA International Conference on Spacecraft Guidance, Navigation and Control System*, Noordwijk, The Netherlands.

Czopek, F. M. and Shellenberger, S. (1993). Description and Performance of the GPS Block I and II L-Band Antenna and Link Budget. *Proceedings of ION GPS 93*, Salt Lake City, Utah.

Falcone, M., Lugert, M., Malik, M., Crisci, M., Rooney, C. E., Jackson, C. and Trethewey, M., ''Giove-A In Orbit Testing Results'', ION GNSS 2006, Fort Worth, TX, September 26–29, 2006.

Moreau, M. C., Axelrad, P., Garrison, J. L. and Long, A. (2000). GPS Receiver Architecture and Expected Performance for Autonomous Navigation in High Earth Orbits. *Navigation*, Vol. 47, No. 3, pp. 191–204.

Moreau, M. C., Davis, E. P., Carpenter, J. R., Kelbel, D., Davis, G. W. and Axelrad, P. (2002). Results from the GPS flight Experiment on the High Earth Orbit AMSAT OSCAR-40 Spacecraft. *Proceedings of ION GPS 2002*, Portland, Oregon.

Powell, T. D., Martzen, P. D., Sedlacek, S. B., Chao, C., Silva, R., Brown, A. and Belle, G. (1999). GPS Signals in a Geosynchronous Transfer Orbit: Falcon Gold Data Processing. *Proceedings of ION National Technical Meeting*, San Diego, California.

Rooney, E., Paffett, J., Unwin, M. and Garutti, A. (2004). Status of GSTB-V2/A Satellite Programme, *Proceeding of ION GNSS 2004*, Long Beach, California.

Steenwijk, R. de Vos Van, Unwin, M. J., Hashida, Y., Blunt, P., Weiler, R., Navitec 2006, 11–13 December 2006, ESA/Estec, Noordwijk.

Underwood, C., Unwin, M. J., Sorensen, R. H., Frydland, A. and Jameson, P. (2004). Radiation Testing Campaign for a New Miniaturised Space GPS Receiver. *Proceedings of IEEE Nuclear and Space Radiation Effects Conference*, Atlanta, Georgia.

Unwin, M. J. and Oldfield, M. K. (2000). The Design and Operation of a COTS Space GPS Receiver, *Proceedings of the 23rd Annual AAS Guidance and Control Conference*, Breckenridge, Colorado.

Winternitz, L., Moreau, M. and Boegner, G. J. (2004). Navigator GPS Receiver for Fast Acquisition and Weak Signal Space Applications. *Proceedings of ION GNSS 2004*, Long Beach, California.